THEMIS ROTO IMAGES: A UNIQUE OFF-AXIS DATASET FOR DETERMINING SURFACE ROUGHNESS CHARACTERISTICS

McKeeby, B.E., Ramsey, M.S. and Simurda, C.M.

Dept. of Geology and Environmental Science, Univ. of Pittsburgh, 4107 O'Hara Street, Pittsburgh, PA, 15260 (bem101@pitt.edu)

Introduction:

Thermal infrared (TIR) spectra are influenced by a number of surficial and atmospheric properties. After correction for the atmosphere; surface roughness, composition, and temperature govern spectral morphology. On planetary surfaces, sub-pixel surface roughness produces shadowing, thermal mixing, and potential changes to the emission spectrum. This is commonly seen as a negative spectral slope at longer wavelengths that could result in incorrect compositional analysis. Non-nadir emission measurements provide unique data on surface roughness, emission phase functions and small-scale slopes [1]. These changes to emissivity data at longer wavelengths have been studied using TES data of select regions on Mars (including areas south of Arsia Mons). The surfaces of these regions were shown to have the largest RMS roughness values on the planet at the TES spatial scale [1,2]. For this study, we utilize the smaller spatial scale of THEMIS data to detect possible surface roughness at the sub-meter scale. Using the unique Routine Off-nadir Targeted Observations (ROTO) data, made possible by the off-axis rotation of the Mars Odyssey spacecraft, we investigate the effects of this sub-pixel surface roughness and temperature on the emissivity spectra. This approach is complementary to the work of Bandfield & Edwards [1], exploring one of their high roughness targets (Daedalia Planum), but using higher spatial resolution data acquired from off-nadir vantage points.

Location:

A ROTO image triplet was acquired of the flow field in Daedalia Planum, southwest of Arsia Mons (-24° 21' 28"N; -122° 37' 47") (Table 1). This flow field was targeted because of the prior roughness studies, but also for its relatively young age (~100 Mya) and the unusual thermophysical variations [3-7]. A crater within this flow field was also examined to further emphasize the effects of a changing emission angle (as a function of crater wall slope).

Procedure:

Atmospherically-corrected, calibrated IR radiance data using the THEMIS standard processing [8] were acquired from the archive at ASU. These IR radiance data were converted to emissivity using emissivity normalization [9]. Individual study sites including craters (Figs. 1-2) and lava flows (Figs. 2-3) were chosen based on observed differences between the ROTO images (Fig. 2C). This image (THEMIS nadir b6/ off-nadir b9) highlights the subtle spectral variation due to possible roughness. Averaged emissivity spectra from regions of interest (ROI) of four THEMIS pixels in size were extracted for each study site. ROTO images acquired at -25˚ off-nadir and nadir were then examined to determine the effects of changing emission angle and roughness detection on surface emissivity. These sites were also examined in HiRISE and CTX data (Fig. 3) for visible roughness variations.

ID Number	Angle	Year	Solar Longitude	Local time (24 hours)
I68222002	Nadir	33	357.92˚	17.95
I68172002	-25˚	33	355.85˚	17.70
I68197002	-13˚	33	356.89˚	17.82

Table 1. THEMIS image identification and collection parameters.

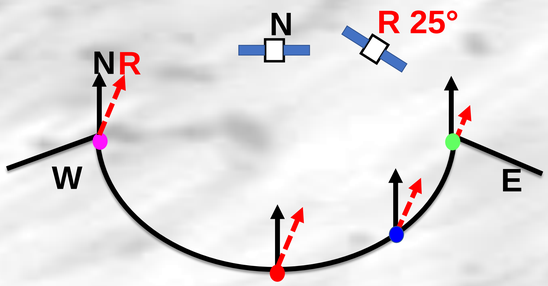

Figure 1. Conceptual drawing of the crater showing viewing geometry and ROI locations of emissivity spectra. Size of the red vectors indicate the magnitude of observed emission.

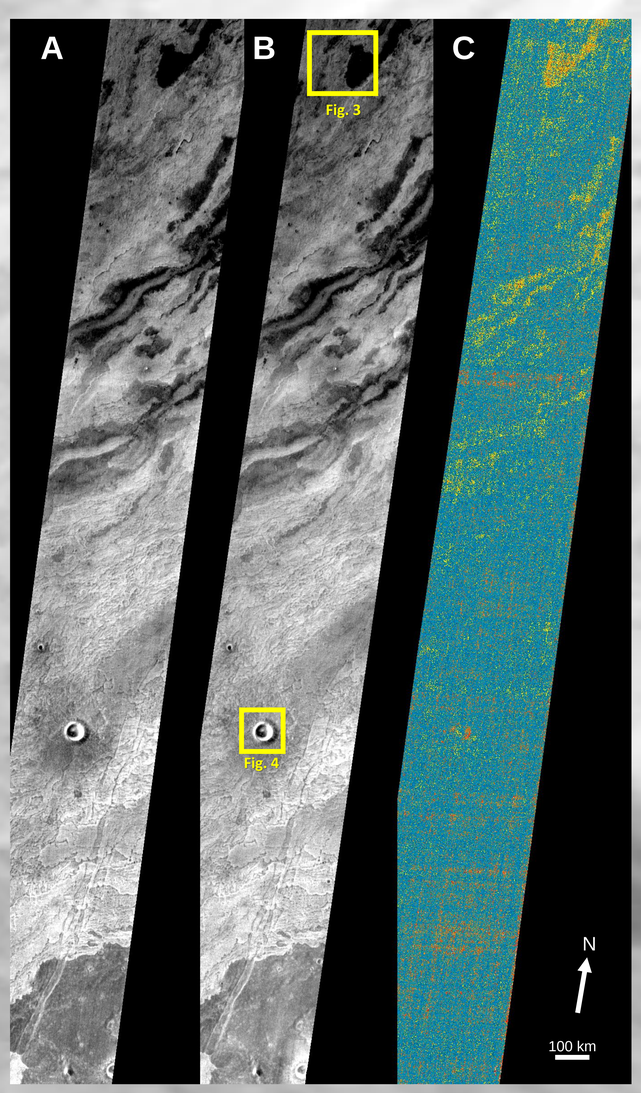

Figure 2. THEMIS band 9 radiance shown at the **(A)** nadir and **(B)** off-nadir (-25˚) viewing angles. **(C)** Emissivity difference image (nadir band 9 / off-nadir band 6). Yellow boxes indicate figure locations.

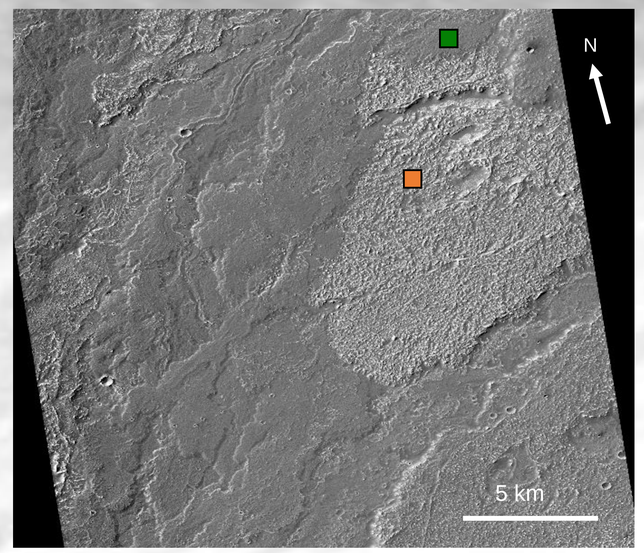

Figure 3. CTX image (B17_016411_1594_XN_20S122W) of the volcanic flow field to the south of the Arsia Mons and north of study crater. ROI locations are indicated by the orange and green boxes.

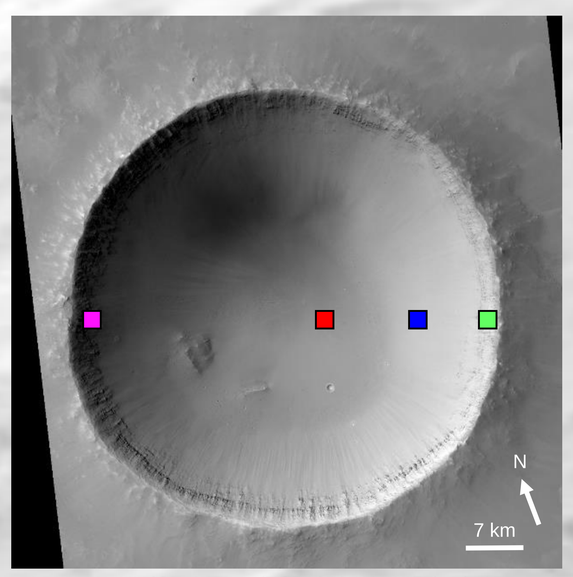

Figure 4. HiRISE image (ESP_050511_1555) of the study crater with ROI locations shown by colored boxes. The emission angle of the magenta ROI will be closer to normal viewing geometry with respect to off-nadir geometry compared to that of the green ROI. The study crater is 39 km wide.

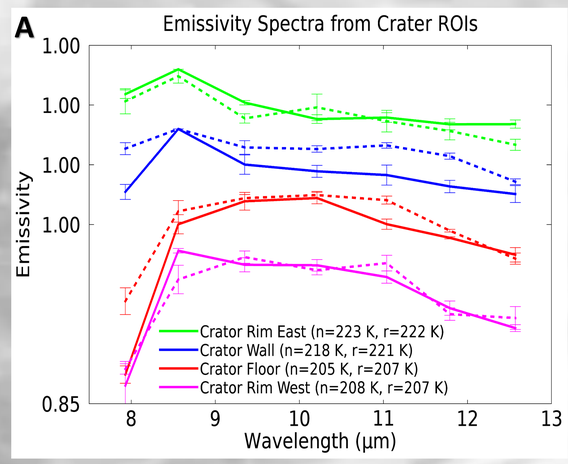

Figure 5. **(A)** Nadir and -25° off-nadir ROTO spectra for 4 locations on different crater slopes. Colors correspond to locations in Figs. 1 and 4. **(B)** Emissivity spectra from the volcanic flow field (colors correspond to the ROI's in Fig. 3). For both plots dashed lines indicate off-nadir observations and solid lines indicate nadir observations. Standard deviation with 2-sigma uncertainty is shown for all spectra, with **n** indicating nadir temperatures and **r** indicating off-nadir temperatures.

Initial Results:

- The target crater appears dusty in HiRISE data with relatively featureless walls, which is reflected in the overall shape of the emissivity spectra (Figs. 4, 5A) [10].
- These crater spectra are indicative of dust and show little variation at the different ROI locations.
  - The subtle changes between the nadir and off-nadir spectra also indicate a surface dominated by dust with very little sub-pixel roughness variability.
  - The long wavelength decrease in emissivity of the eastern slope ROI (magenta) compared to the western slope ROI (green) does possibly indicate more sub-pixel roughness/shadowing caused by the topographic slope combined with the emission angle.
  - Emissivity changes in the crater are therefore dominated mostly by the changing emission angle as a function of the crater slope except at the uppermost crater rim (Figs. 1, 4, 5A).
- The emissivity spectra of the volcanic flow field show a larger difference between the nadir and off-nadir data.
  - These spectra also have a larger long wavelength negative slope indicative of sub-pixel shadowing caused by rougher surfaces.
  - This negative slope is more pronounced in the blockier, channelized flows similar to a'a (Fig. 5B).
  - However, off-nadir observations also show slightly higher temperatures (1-4˚C), which is not consistent with sub-pixel shadowing and must be investigated.
- Fine particles (i.e., dust) on these flows will also reduce the spectral contrast similar to the study crater (Fig. 5A).

Summary:

Initial analysis of the THEMIS ROTO data show subtle to more pronounced changes in emissivity between the viewing angles for all ROIs. A loss in spectral contrast is observed between nadir and off-nadir observations on the volcanic flow field as well as between the different flow morphologies (smooth vs. rough flows). This can be explained by changes in surface slope and roughness.

Future Work:

Further analysis is needed to quantify the observed spectral and temperature variations and link the results to prior modeling studies [1,2]. ROTO data will be combined with a HiRISE DEM to quantify the scales of roughness. These data will also be compared with the Θ-bar surface slope distribution model to investigate whether this dataset is able to determine precise surface roughness at a sub-pixel (TES) scale and validate those results [11]. If so, the results can be combined with high-resolution image data and DEM to quantify surface morphology with unit age and regional geology. We also propose to expand ROTO collections to other areas indicative of roughness variability and rover locations where in-situ surface observations are available.

Acknowledgements:

The authors would like to thank the THEMIS Science and Odyssey Mission teams for their continued support and acquisition of the ROTO data, as well as James Thompson for his assistance with the spectral plots.

References:

[1] Bandfield, J.L. and Edwards, C.S. (2008) *Icarus, 193,* 139–157. [2] Bandfield, J.L. et al. (2009) *Icarus, 202,* 414-428. [3] Simurda, C.M. et al (2018), *LPSC XLIX* Abstract # 1792. [4] Ramsey, M.S. and Crown, D.A. (2010) *LPSC XLI*, Abstract # 1111. [5] Ramsey, M.S. and Crown, D.A. (2017) *JVGR*, *342*, 13-28. [6] Crown, D.A. et al (2015) *LPSC XLVI*, Abstract # 1439. [7] Crown, D.A. et al (2010) *LPSC XLI*, Abstract # 2225.[8] Christensen, P.R. Mars Odyssey THEMIS: Data Processing User's Guide. [9] Realmuto, V.J. (1990) JPL Pub. 90-55, 31-35. [10] Bell, et al. (1993) *JGR*, 98, 3372-3385.n [11] Hapke, B. (1984) *Icarus*, *59*, 41-59.